PHYSICAL REVIEW B VOLUME 52, NUMBER 16 15 OCTOBER 1995-II

Chemical hardness, linear response, and pseudopotential transferability

A. Filippetti
Istituto Nazionale di Fisica della Materia and Dipartimento di Scienze Fisiche, Università di Cagliari, Via Ospedale 72, I-09124 Cagliari, Italy

David Vanderbilt, W. Zhong, and Yong Cai*
Department of Physics and Astronomy, Rutgers University, Piscataway, New Jersey 08855-0849

G.B. Bachelet
Dipartimento di Fisica, Università di Roma La Sapienza, Roma, Italy
(Received 8 May 1995; revised manuscript received 25 July 1995)

We propose a systematic method of analyzing pseudopotential transferability based on linear-response properties of the free atom, including self-consistent chemical hardness and polarizability. Our calculation of hardness extends the approach of Teter not only by including self-consistency, but also by generalizing to nondiagonal hardness matrices, thereby allowing us to test for transferability to nonspherically symmetric environments. We apply the method to study the transferability of norm-conserving pseudopotentials for a variety of elements in the Periodic Table. We find that the self-consistent corrections are frequently significant, and should not be neglected. We prove that the partial-core correction improves the pseudopotential hardness of alkaline metals considerably. We propose a quantity to represent the average hardness error and calculate this quantity for many representative elements as a function of pseudopotential cutoff radii. We find that the atomic polarizabilities are usually well reproduced by the norm-conserving pseudopotentials. Our results provide useful guidelines for making optimal choices in the pseudopotential generation procedure.

I. INTRODUCTION

Density-functional calculations performed within the framework of the local-density approximation (LDA) have been demonstrated to give accurate predictions of many physical properties of solids.[1] The introduction of the pseudopotential approximation greatly simplifies electronic-structure calculations by eliminating the need to include atomic core electrons and the strong potentials responsible for binding them.[2] The introduction of norm-conserving pseudopotentials by Hamann, Schlüter, and Chiang[3] (HSC) led to greatly improved control of transferability errors, and as a result the pseudopotential approach has since found a wide range of applications in molecular and solid-state electronic-structure theory. Nevertheless, transferability is still an issue in many calculations, especially when uncomfortably large pseudopotential cutoff radii have been dictated by the requirements of a modest plane-wave cutoff in the solid-state calculation, and for atoms having shallow core shells.

A pseudopotential (PSP) is constructed to replace the all-electron (AE) atomic potential in such a way that core states are eliminated. The most important measure of a pseudopotential is its transferability, which characterizes the accuracy with which it mimics the real AE atom in different atomic, ionic, molecular, or solid-state environments. Traditionally, the transferability of a pseudopotential is characterized by two properties: (i) a comparison of the scattering properties of the AE and PSP versions of the free atom or ion, as measured by the logarithmic derivative of the wave function at some diagnostic radius as a function of energy; and (ii) configuration tests, which check if the pseudoeigenvalues and total energies track the AE ones for various excited states of the free atom or ion. It is important to note that spherical symmetry is implicit in both of these approaches, so that neither is capable of giving information about transferability to anisotropic environments.

Scattering properties are certainly a significant aspect of transferability: poor scattering properties are indicative of a poor pseudopotential. A major contribution of HSC was to show that the norm-conserving condition automatically implies that not only the logarithmic derivative, but also its energy derivative, is guaranteed to be correct for the PSP at a reference energy, thus insuring that the AE and PSP scattering properties will match closely over a large energy range.[3] Thus, norm-conserving potentials tend to have much better transferability for most elements. However, the matching of logarithmic derivatives is not always sufficient to ensure good transferability. Some potential sources of error that will not show up in tests of scattering properties are (i) electrostatic screening effects, and (ii) effects of nonlinearity of the exchange-correlation energy (important for many alkali-metal elements). Errors of the former type are usually easily eliminated by the choice of a "conservative" cutoff radius,[4,5] while those arising from core-valence overlap can largely be corrected by use of the frozen-core correction.[6] Nevertheless, these examples illustrate the dangers of focusing on scattering properties alone.

0163-1829/95/52(16)/11793(12)/$06.00

Configuration tests are certainly useful as a supplementary criterion, but as mentioned above, they do not control the quality of the PSP in a nonspherical target environment. This will obviously be important for atoms in surface, defective, molecular, or liquid environments, to name just a few. Furthermore, it is difficult to include the configuration tests systematically as part of the PSP generation procedure.

As LDA calculations are pushed in the direction of high accuracy, PSP errors become less tolerable, putting tight requirements on transferability. On the other hand, as the calculations are pushed to larger system sizes, the increased computational load requires that the PSP be as smooth (soft) as possible. This has led to a tremendous effort to optimize PSP softness.[7–9] Unfortunately, transferability and softness are usually contradictory requirements. Especially for first-row elements, attempts to save computational cost frequently result in the use of a PSP with an uncomfortably large core cutoff radius. Because of the above-mentioned electrostatic screening problems, this strategy may result in a sacrifice of transferability, which would be difficult to detect using the conventional methods. It is therefore of great importance to develop improved measures of transferability that will allow for improved control of PSP errors in cases like these. It is especially desirable to develop methods that work directly at the atomic level, without the need for painstaking comparisons of pseudo and AE results in molecular and solid-state environments.

In this paper, we propose to use the linear-response properties of a reference free atom or ion as a measure of the transferability of a PSP. We calculate two kinds of linear-response properties: a generalized chemical hardness, and the dipole and higher-moment susceptibilities. Chemical hardness measures the derivatives of electronic eigenvalues with respect to changes of occupation. It was recently proposed by Teter[10] as an important measure of PSP transferability, partly based on the idea that the chemical potential and hardness have equal roles in determining electron charge transfers. To some extent, the hardness analysis is redundant with configuration tests (of which it is a kind of differential version), but it is more systematic and can be incorporated into PSP generation more easily.[10] The concept of hardness is generalized in this paper to include also information about the response to nonspherical perturbations. This is in fact very important, and we shall see that the rearrangement of charge in a p shell may dominate the error in the hardness matrix. We further include the self-consistent change of the wave functions in our calculations in order to go beyond the frozen-wave-function approximation (FWA) introduced by Teter.[10] Finally, the dipole (and quadrupole, etc.) susceptibility tests measure the ability of the pseudoatom to imitate the correct AE behavior in a local electric field (or field gradient, etc.), which may result from an anisotropic solid-state or molecular environment.

This paper is arranged as follows. In Sec. II we review the concept of chemical hardness and introduce the formulation for calculating both spherical and nonspherical hardness. We also outline the calculation of the dipole and higher-order polarizabilities. In Sec. III, we present calculated chemical hardness matrices and polarizabilities for some representative atoms chosen from different parts of the Periodic Table. We discuss the general trends in the hardness matrix, and the effect of the frozen-core correction. We also proposed a quantity based on the hardness matrix to characterize the pseudopotential transferability. Finally, we conclude our results in Sec. IV.

II. THEORY

A. Chemical hardness

Teter defines the chemical hardness matrix H_{ij} within the LDA as[10]

$$H_{ij} = \frac{1}{2}\frac{\partial^2 E[\rho]}{\partial f_i \partial f_j} , \tag{1}$$

where E is the Janak functional[11] and f_i is the occupation number of the ith state. Since the eigenvalue $\epsilon_i = \partial E/\partial f_i$, we have

$$H_{ij} = \frac{1}{2}\frac{\partial \epsilon_i}{\partial f_j} . \tag{2}$$

Thus, the hardness matrix measures the first-order change of an energy eigenvalue resulting from a first-order variation of an occupation number, while allowing the total number of electrons to vary. Application of the Hellmann-Feynman theorem to Eq. (2) yields

$$\begin{aligned} H_{ij} &= \frac{1}{2}\left\langle \psi_i \left| \frac{\partial}{\partial f_j}[T + V_{\text{ion}} + V_{\text{hxc}}] \right| \psi_i \right\rangle \\ &= \frac{1}{2}\left\langle \psi_i \left| \frac{\partial V_{\text{hxc}}}{\partial \rho}\frac{\delta \rho}{\delta f_j} \right| \psi_i \right\rangle . \end{aligned} \tag{3}$$

The term $\delta\rho/\delta f_j$ consists of two parts: one due to the change of the screening potential with variation of the occupation number for fixed wave functions, and one arising from relaxation of the wave functions. Teter made the approximation of omitting the second term, but both are included here.

Frequently, one is interested only in the case where the occupations of the states comprising a given shell are kept equal. For example, one may consider an excitation in which one transfers an s electron to the p shell, increasing the occupation of each p state by 1/3. This ensures retention of spherical symmetry of the charge density and potential, and is implicit in all of the analysis, which is usually carried out with an atomic pseudopotential program. In this case, different m components remain degenerate and the treatment is simple.[10] In real situations (in molecules, at surfaces, etc.), atoms may have very anisotropic environments, so that nonspherical changes of electron occupation become important. This prompts us to consider also changes of occupation, which lead to nonspherical changes of density and screening potential. We will use the index L to refer to density or potential changes having angular character $Y_{LM}(\Omega)$.

Thus, we shall not restrict ourselves to spherically symmetric ($L = 0$) perturbations, but will consider the general $L \neq 0$ case.

For this purpose, it is useful to generalize from the concept of an occupation number f_i to the concept of an "occupation matrix" or "density matrix" f_{ij}, to be defined shortly in Eq. (5). This generalization, previously introduced in other contexts,[12,13] makes the hardness analysis more complete. While f_{ij} is diagonal in the atomic ground state, or in a basis of energy eigenstates of a perturbed system, it may be nondiagonal in a more general representation of a perturbed system such as an atom in a defective environment.

In our calculations, we use first-order density-functional perturbation theory in the framework of LDA, following the scheme formulated by Mahan and Subbaswamy.[14] In the remainder of this section, we will give a detailed formulation of the calculation of the generalized hardness matrix elements with general occupation matrix f_{ij}. Both the FWA and the full self-consistent hardness are to be discussed. Then, we sketch the calculation of the dipole and higher susceptibilities, which is straightforward after the machinery needed to calculate the hardness elements has been set up. All the energies are expressed in Rydberg units.

B. Generalized hardness

The ground-state atomic charge density $n(\mathbf{r})$ of a system can be expressed using occupation numbers f_i through

$$\rho(\mathbf{r}) = \sum_i f_i \, |\psi_i(\mathbf{r})|^2 \, . \tag{4}$$

However, if one wants to express a perturbed or excited atomic charge density in terms of (both filled and empty) Kohn-Sham orbitals of a reference ground-state atom, then, in general, the occupation numbers turn out to be nondiagonal, so that the total charge density should be expressed as

$$\rho(\mathbf{r}) = \sum_{ij} f_{ij} \, \psi_i^*(\mathbf{r}) \psi_j(\mathbf{r}), \tag{5}$$

where $f_{ij} = f_i \delta_{ij}$ only in the ground state. The most general result of a perturbation is thus obtained by allowing for nondiagonal terms f_{ij} to exist.[12,13] Taking this into account, we arrive at a more general form of the hardness matrix. As we shall see, this provides a natural way to test the transferability of a PSP to nonspherical environments.

We assume spherical symmetry of the unperturbed reference atom. Instead of working in the explicit atomic representation $f_{ij} = f_{nlm,n'l'm'}$, we find it convenient to work in a representation $(nn'll'LM)$ in which LM are labels of total angular momentum, and $L = |l - l'|, |l - l'| + 2, \ldots, l + l'$ following the usual angular-momentum addition rules. Introducing the condensed notation $\alpha = nn'll'$, we have

$$\rho(\mathbf{r}) = \sum_{\alpha LM} f_{\alpha LM} \, n_{\alpha LM}(\mathbf{r}) \, . \tag{6}$$

Here

$$f_{\alpha LM} = \sum_{mm'} C(LM; lm, l'm') f_{nlm,n'l'm'}, \tag{7}$$

with $C(LM; lm, l'm')$ being the Clebsch-Gordon coefficients, and $n_{\alpha LM}(\mathbf{r}) = n_\alpha(r) \, Y_{LM}(\Omega)$ with $n_\alpha(r) = R_{nl}(r) R_{n'l'}(r)$. In this notation, it is natural to introduce the generalized Kohn-Sham eigenvalues

$$\epsilon_{\alpha LM} = \frac{\partial E}{\partial f_{\alpha LM}} \tag{8}$$

and the generalized hardness matrix

$$H_{\alpha\beta LL'MM'} = \frac{1}{2} \frac{\partial^2 E}{\partial f_{\alpha LM} \, \partial f_{\beta L'M'}} \, . \tag{9}$$

Within the framework of LDA, application of Eq. (3) to the latter yields

$$H_{\alpha\beta LL'MM'} = \frac{1}{2} \int\int d\mathbf{r} \, d\mathbf{r}' \, n_{\alpha LM}(\mathbf{r}) \, w_{\mathrm{hxc}}(\mathbf{r}, \mathbf{r}') \times \frac{\delta\rho(\mathbf{r}')}{\delta f_{\beta L'M'}} \, . \tag{10}$$

Here, the kernel is

$$w_{\mathrm{hxc}}(\mathbf{r}, \mathbf{r}') = \frac{\partial V_{\mathrm{hxc}}(\mathbf{r})}{\partial \rho(\mathbf{r}')} \, , \tag{11}$$

with $V_{\mathrm{hxc}}(\mathbf{r})$ being the Hartree and exchange-correlation potential.

We now make use of the spherical symmetry of the unperturbed reference configuration. The eigenvalue $\epsilon_{\alpha LM}$ is then only nonzero for $L = M = 0$ and $n = n'$, $l = l'$. As for the hardness matrix, the spherical symmetry implies

$$H_{\alpha\beta LL'MM'} = H_{\alpha\beta L} \, \delta_{LL'} \, \delta_{M,-M'} \, . \tag{12}$$

Moreover, w_{hxc} can be decomposed into angular and radial terms as

$$w_{\mathrm{hxc}}(\mathbf{r}, \mathbf{r}') = \sum_{LM} w_{\mathrm{hxc}}^{(L)}(r, r') \, Y_{LM}^*(\Omega) \, Y_{LM}(\Omega') \, , \tag{13}$$

where

$$w_{\mathrm{hxc}}^{(L)}(r, r') = \frac{8\pi}{2L+1} \frac{r^{<L}}{r^{>L+1}} + \frac{\delta V_{\mathrm{xc}}}{\delta n(r)} \frac{\delta(r - r')}{r^2} \tag{14}$$

and $r^<$ and $r^>$ are the smaller and larger of r and r', respectively. Note that the exchange-correlation term, being local, is independent of L. Thus, $H_{\alpha\beta L}$ in Eq. (12) becomes

$$H_{\alpha\beta L} = \frac{1}{2} \int\int dr \, dr' \, r^2 \, r'^2 \, n_\alpha(r) \, w_{\mathrm{hxc}}^{(L)}(r, r') \, \frac{\delta\rho(r')}{\delta f_\beta} \, . \tag{15}$$

The density variation due to the variation of occupation numbers consists of two terms:

$$\frac{\delta\rho(r)}{\delta f_\alpha} = n_\alpha(r) + \Delta n_\alpha(r) \ . \tag{16}$$

The first term arises from the explicit dependence of density on the occupation numbers, while the second involves relaxation of the wave function with changes of occupation. We will refer to the neglect of Δn_α as the FWA, while the effect of the Δn_α term will be referred to as the "self-consistency" (SC) correction. The FWA part of the hardness matrix is relatively easy to calculate, and its diagonal case has previously been done for almost all atoms in the Periodic Table.[15] The SC correction is treated using density-functional linear-response theory, regarding the change of f_α as an external perturbation.

We start with the calculation of the FWA hardness. From Eqs. (15) and (16), it is easy to see that it may be written as

$$H^{\rm FWA}_{\alpha\beta L} = \frac{1}{2}\int\int dr\, dr'\, r^2\, r'^2\, n_\alpha(r)\, w^{(L)}_{\rm hxc}(r,r')\, n_\beta(r') \tag{17}$$

$$= \frac{1}{2}\int dr\, r^2 v^{(L)}_\alpha(r)\, n_\beta(r) \ , \tag{18}$$

where $v^{(L)}_\alpha$ is the linear-order change of potential due to the FWA variation of density with respect to $f_{\alpha LM}$. It is given by

$$v^{(L)}_\alpha = \int dr'\, r'^2\, w^{(L)}_{\rm hxc}(r,r')\, n_\alpha(r') \ . \tag{19}$$

The SC correction to the hardness arises because the presence of $v^{(L)}_\alpha(r)$ induces a change $\Delta n_\alpha(r)$ in the charge density. The latter is computed self-consistently, treating $v^{(L)}_\alpha(r)$ as though it were a bare potential perturbation. According to a theorem by Eaves and Epstein,[16] for a closed-shell atom, the first-order induced charge density has the same angular character as the perturbing potential. Within LDA (with spin-polarization neglected) the ground state is always isotropic (equal population of each m character of any given shell), so this theorem applies. To linear order, we can write

$$\Delta n^{(L)}_\alpha(r) = \int dr'\, r'^2\, \chi^{(L)}(r,r')\, v^{(L)}_\alpha(r') \ , \tag{20}$$

where $\chi^{(L)}(r,r')$ is the linear susceptibility in radial coordinates for perturbations of angular character L. Thus, the self-consistent correction is given by

$$\Delta H^{\rm SC}_{\alpha\beta L} = \frac{1}{2}\int\int dr\, dr'\, r^2\, r'^2\, v^{(L)}_\alpha(r) \times\chi^{(L)}(r,r')\, v^{(L)}_\beta(r') \ . \tag{21}$$

The determination of the linear susceptibility $\chi^{(L)}(r,r')$ follows closely the modified Sternheimer approach discussed by Mahan and Subbaswamy.[14] In what follows, we consider the density response $\Delta n^{(L)}(\mathbf{r}) = \Delta n^{(L)}(r) Y_{L0}(\Omega)$ to a general perturbation $v^{(L)}(\mathbf{r}) = v^{(L)}(r) Y_{L0}(\Omega)$ of angular character L. (We have $v = v^{(L)}_\alpha$ and $\Delta n = \Delta n^{(L)}_\alpha$ in the immediate context, where α is the index of the state whose occupation is being varied. However, the discussion given below is general, and the indices nlm will henceforth be taken to refer to arbitrary occupied wave functions that respond to the perturbation.) We do not actually need to calculate χ itself; instead, it is sufficient to specify an iterative algorithm for calculating its action upon the arbitrary perturbation [Eq. (20) in our case].

The procedure is as follows. For the moment, we assume that the first-order density change $\Delta n^{(L)}(r)$ is known. The corresponding change $\Delta v^{(L)}_{\rm scf}(r)$ in the screened Kohn-Sham potential is then given by

$$\Delta v^{(L)}_{\rm scf}(r) = v^{(L)}(r) + \int dr'\, r'^2\, w^{(L)}_{\rm hxc}(r,r')\, \Delta n^{(L)}(r') \ . \tag{22}$$

This induces a first-order change in each Kohn-Sham wave function satisfying

$$(\mathcal{H}_0 - \epsilon_{nl})\, \Delta\psi_{nlm} = -\left(\Delta V^{(L)}_{\rm scf} - \Delta\epsilon_{nlm}\right)\psi_{nlm} \ , \tag{23}$$

where $\mathcal{H}_0, \epsilon_{nl}$, and $\psi_{nlm}(\mathbf{r})$ are the unperturbed Kohn-Sham Hamiltonian, eigenvalue, and eigenfunction, respectively, while $\Delta\epsilon_{nlm}$ and $\Delta\psi_{nlm}(\mathbf{r})$ are the corresponding first-order changes. Decomposing Eq. (23) into angular and radial parts, one finds

$$\Delta\psi_{nlm}(\mathbf{r}) = \sum_{l'=|l-L|}^{l+L} C(L0; lm, l'm)\Delta R_{nll'}(r) Y_{l'm}(\Omega) \ , \tag{24}$$

where the $C(L0; lm, l'm)$ are Clebsch-Gordon coefficients and the radial functions $\Delta R_{nll'}(r)$ are the solutions of the radial part of Eq. (23),

$$\left[-\frac{d^2}{dr^2} + \frac{l'(l'+1)}{r^2} + V_{\rm ion}(r) + V_{\rm hxc}(r) - \epsilon_{nl}\right]\Delta R_{nll'}(r)$$

$$= [\Delta\epsilon_{nlm} - \Delta v_{\rm scf}(r)]\, R_{nl}(r) \ . \tag{25}$$

This inhomogeneous equation is solved numerically on a radial mesh following Ref. 14. Finally, the change of density resulting from Eq. (24) is

$$\Delta n^{(L)}(r) = \sum_{n,l,l'} \frac{f_{nl}}{2(2l+1)}\Delta R^{(L)}_{nll'}(r)\, R_{nl}(r) D(ll', L) \ , \tag{26}$$

where $f_{nl} = \sum_m f_{nlm}$ and $D(ll', L) = \sum_m C^2(L0; lm, l'm)$. Iterative solution of Eqs. (22), (25), and (26) thus gives the self-consistently screened density change $\Delta n^{(L)}(r)$ resulting from the perturbation $v^{(L)}(r)$ in Eq. (20).

Before closing this subsection, we comment briefly on the case of diagonal hardness, $f_{ij} = f_i\delta_{ij}$, so that one considers only conventional occupation numbers $f_i = f_{nlm}$. The hardness matrix is then

$$H_{\substack{nlm \\ n'l'm'}} = \frac{1}{2}\frac{\partial^2 E}{\partial f_{nlm}\,\partial f_{n'l'm'}} . \tag{27}$$

Since the charge density associated with ψ_{nlm} has angular character $|Y_{lm}(\Omega)|^2 = \sum_{L=0}^{2l} C(L0;lm,lm)\,Y_{L0}(\Omega)$, with L even, one finds

$$H_{\substack{nlm \\ n'l'm'}} = \sum_{L=0}^{2l_{\min}} C(L0;lm,lm)\,C(L0;l'm',l'm')\,H_{\alpha\beta L} . \tag{28}$$

Here the sum is over even L only, $l_{\min}$ is the smaller of l and l', $\alpha = nnll$, $\beta = n'n'l'l'$, and $H_{\alpha\beta L}$ are given by Eq. (15). Thus, all of the diagonal hardness matrix elements are contained as special cases of the generalized nondiagonal ones introduced earlier. Similar equations relate the FWA and SC contributions separately. Note that the diagonal formulation only covers variations of the screening potential or density of even L (monopole, quadrupole, etc.), whereas the generalized formulation is capable of treating variations of any angular character. In fact, perturbations of dipole ($L = 1$) character are likely to be the most important nonspherical perturbations in many molecular and solid-state environments, especially at surfaces and other defects where inversion symmetry is lacking. Therefore, in what follows we will concentrate on comparisons of the AE and PSP nondiagonal hardness elements $H_{\alpha\beta L}$, with special emphasis on the $L = 0$ and $L = 1$ cases.

C. Polarizability

The polarizability of an atom measures its response to an external electric field. The dipole ($L = 1$), quadrupole ($L = 2$), and higher ($L > 2$) polarizabilities are defined as the derivatives of the Lth induced charge moment with respect to an electrostatic potential of form $r^L Y_{L0}(\Omega)$. For good transferability, it is important that the pseudoatom have polarizabilities similar to those of the all-electron atom. We can expect the lower-moment polarizability to be more important, so we focus on the dipole and quadrupole susceptibility in what follows. Tests of the non-self-consistent polarizability of HSC pseudopotentials have previously been performed for a large number of closed-shells atoms and ions by Bachelet *et al.*[17] Here, we extend the tests to other atoms and also include the SC correction.

The formulation and calculation of the polarizability is straightforward[14,18] using the machinery developed in the previous subsections. The perturbing potential is taken to have the form

$$V_L(\mathbf{r}) = r^L Y_{L0}(\Omega) , \tag{29}$$

and the linearly induced density change is

$$\Delta n^{(L)}(r) = \int dr'\, r'^{L+2}\,\chi^{(L)}(r,r') . \tag{30}$$

This is evaluated using the same iterative procedure given previously in Eqs. (22)–(26). The polarizability in angular channel L is then

$$p_L = -\frac{8\pi}{2L+1}\int dr\, r^{L+2}\,\Delta n^{(L)}(r) , \tag{31}$$

with p_1 and p_2 being the dipole and quadrupole susceptibility, respectively.

III. RESULTS

In this part, we present our calculated hardness matrix elements for a set of representative atoms. We begin with all-electron atoms, surveying the characteristics of the hardness matrix and the basic trends as a function of position in the Periodic Table. We concentrate first on argon, making the comparison between the AE and PSP hardness matrix, discussing sources of error, and introducing our format for presenting results in a systematic fashion. Next, we discuss trends as one goes across the Periodic Table, and evaluate the importance of the Louie-Froyen-Cohen[6] (LFC) semi-core correction and the effects of varying the core radius. We will then propose a method to extract the most important information from the large number of hardness elements. Finally, the calculated AE and PSP polarizabilities will be presented at the end of this section.

The results reported here are restricted to potentials of the HSC type. We believe that these results can be taken as indicative for the whole class of norm-conserving HSC-like PSP's,[3,4,7–9,19] provided comparable cutoff radii are chosen. For Kleinman-Bylander,[20] ultrasoft,[21] or other approaches to PSP construction that deviate significantly from the original HSC method, addition investigation may be appropriate.

A. Hardness matrix for all-electron atoms

Before studying the transferability of PSP's with reference to the hardness matrix elements H_{ij}, we first need to understand the behavior of H_{ij} for all-electron atoms in order to obtain some physical intuition. In Table I, we show some matrix elements of the generalized hardness for three characteristic AE atoms in the Periodic Table. Silicon and argon are taken in the ground-state neutral configuration, while for sodium we choose an ionized valence configuration $3s^{0.5}3p^{0.25}$ in order to ensure that the p electron is bound. The total self-consistent hardness $H^{\text{total}} = H^{\text{FWA}} + H^{\text{SC}}$ is broken down into frozen-wave-function approximation and self-consistent-correction pieces as discussed in the previous section. For some elements, the FWA contribution is further separated into Hartree (h) and exchange-correlation (xc) contributions, $H^{\text{FWA}} = H^h + H^{\text{xc}}$. The matrix elements can be identified by quantum numbers $\alpha = n_1 n_1' l_1 l_1'$, $\beta = n_2 n_2' l_2 l_2'$, and L. Since the principle quantum numbers n are obvious in most cases, we will usually omit them and write the indices simply as $l_1 l_1', l_2 l_2'; L$.

From Table I, we see that H^{FWA} typically dominates,

and the self-consistent correction H^{SC} is only about $20-30\,\%$ of H^{FWA}. Nevertheless, this is clearly large enough that complete neglect of H^{SC} is unjustified. It is also obvious from the table that H^{FWA} are mostly positive, while the H^{SC} are negative. For the diagonal elements (e.g., excluding $\{sp, sp; L=0\}$), this can be understood as follows. From Eq. (17), the Hartree part of H^{FWA} can be seen to have the form of the Coulomb self-energy of a particular charge distribution $n_\alpha(r)Y_{LM}(\Omega)$, which must be positive. On the other hand, the exchange-correlation contribution is negative because $\delta V_{\mathrm{xc}}/\delta n$ in Eq. (14) is negative. Typically, the Hartree term dominates and H^{FWA} is positive. Regarding H^{SC}, note that Eq. (21) can be interpreted as evaluating the second-order energy change of the system when the external potential of Eq. (19) is applied; the total energy must go down when the wave functions relax, so that H^{SC} must be negative.

Going from Na to Ar, we find that H^{total} increases strongly, primarily because of the Hartree contribution H^h to H^{FWA}. This is in agreement with our intuition, since the wave functions become much more localized as one moves from left to right across the Periodic Table, causing H^h to increase sharply. In this sense, we can refer to atoms (like Ar) on the right side of the Periodic Table as "strongly electrostatic atoms" or "hard atoms," while those on the left side (like K) can be termed "soft."

TABLE I. Calculated all-electron hardness matrix elements of three representative atoms Na, Si, and Ar. Both frozen-wave-function approximation (FWA) and self-consistent (SC) contributions to the total hardness elements are listed. For some matrix elements, the FWA hardness is broken down into Hartree (h) and exchange-correlation (xc) contributions.

	Na($3s^{0.5}3p^{0.25}$)	Si($3s^23p^2$)	Ar($3s^23p^6$)
$ss, ss; L=0$			
FWA	0.1906	0.3923	0.6142
SC	-0.0166	-0.0931	-0.1684
Total	0.1741	0.2992	0.4457
$ss, pp; L=0$			
FWA	0.1562	0.3437	0.5668
SC	-0.0144	-0.0737	-0.1444
Total	0.1417	0.2700	0.4224
$pp, pp; L=0$			
FWA (h)	0.1625	0.3260	0.5465
FWA (xc)	-0.0374	-0.0197	-0.0197
FWA	0.1251	0.3063	0.5268
SC	-0.0131	-0.0586	-0.1240
Total	0.1120	0.2477	0.4028
$sp, sp; L=1$			
FWA (h)	0.0367	0.0766	0.1275
FWA (xc)	-0.0319	-0.0203	-0.0212
FWA	0.0048	0.0563	0.1063
SC	-0.0014	-0.0306	-0.0560
Total	0.0033	0.0257	0.0504
$pp, pp; L=2$			
FWA (h)	0.0164	0.0321	0.0536
FWA(xc)	-0.0374	-0.0197	-0.0197
FWA	-0.0210	0.0124	0.0339
SC	-0.0031	-0.0018	-0.0068
Total	-0.0242	0.0106	0.0272

Our results also indicate that the matrix elements of H^{total} for $L=0$ are significantly larger than those for $L>0$. This implies that the diagonal hardness elements defined in Eq. (28) are dominated by the spherically symmetric part of the response. A closer inspection reveals that H^h decreases strongly with increasing L, while H^{xc} is smaller and, being a local operator, independent of L. This gives rise to an overall small H^{total} for high L. In a few cases where the valence wave function was very weakly bound and delocalized, we have found that H^{xc} can even be larger in magnitude than H^h, resulting in a small but *negative* H^{total}. We regard this as an unphysical result that reflects the overestimate of exchange-correlation effects by the LDA in the low-density tail of the atom.

B. Argon: AE and PSP hardness

Having gained some understanding of the AE hardness matrix, we turn now to a comparison of the PSP hardness elements with the corresponding AE ones. We begin with argon. In Table II we list values for some important hardness matrix elements calculated for the AE and PSP Ar^+ ion in configuration $s^{1.2}p^{5.7}d^{0.1}$. The HSC PSP was generated in this configuration, using a core radius $r_c \simeq 1$ a.u. We also show the relative errors for another valence configuration, $s^1p^{5.5}d^{0.5}$.

Comparing the AE and PSP results, we find very good agreement for the $L=0$ matrix elements. Norm conservation imposes the constraint that the $L=0$ component of the electrostatic potential in the PSP case should match the AE one outside the core region. Consequently, for small core radii the differences between AE and PSP values of H^h are essentially confined to $L>0$ moments. Actually, we find that the errors in H^h are relatively insensitive to a modest increase of core radius for hard atoms like Ar.

Because of this constraint, while the Hartree contribution is large in magnitude, it may only incur a small error in hardness. For Ar, the H^{xc} are quite small and their contributions to the error are not very significant. So, for Ar, the agreement between AE and PSP hardness elements is excellent in the spherically symmetric ($L=0$) channel. The relative errors for $L>0$ channels are larger ($\sim 20\%$ for $L=1$ and $\sim 4\%$ for $L=2$). However, since their absolute magnitudes are small, they are not as important. As a result, the overall agreement between AE and PSP hardness agrees is very good. We also checked that changing the testing configuration affects the results only very slightly.

In order to avoid presenting numerous cumbersome tables, we have converted the information into the form of a bar chart as shown in Fig. 1. The heights of the bars represent the values of the corresponding hardness matrix elements. The columns indicate different contributions to a given hardness matrix element, whose indices are labeled by the row. The results for AE and PSP atoms are placed side-by-side to facilitate comparison;

hollow bars indicate AE results while dashed bars represent PSP results. The values for $L > 0$ elements, being small, are magnified in the diagram. We believe the discussion is easier to follow by viewing such diagrams, so all subsequent hardness results will be presented in this way.

TABLE II. All-electron (AE) and HSC pseudopotential (PSP) hardness matrix elements for Ar. Two different electronic configurations are considered. The error is the percentage difference between PSP and AE hardness. Total hardness (total) is decomposed into frozen-wave-function approximation (FWA) and self-consistent (SC) contributions, while the FWA is further decomposed into Hartree (h) and exchange-correlation (xc) contributions.

		$s^{1.2}p^{5.7}d^{0.1}$		$s^1p^{5.5}d^{0.5}$
	AE (Ry)	PSP (Ry)	error (%)	error (%)
$ss, ss; L = 0$				
FWA (h)	0.6588	0.6562	0.39	0.41
FWA (xc)	-0.0273	-0.0308	12.98	13.09
FWA	0.6315	0.6254	0.97	1.01
SC	-0.1421	-0.1367	3.80	3.26
Total	0.4894	0.4887	0.15	0.07
$pp, pp; L = 0$				
FWA (h)	0.5876	0.5845	0.53	0.54
FWA (xc)	-0.0230	-0.0254	10.24	10.51
FWA	0.5646	0.5591	0.97	1.00
SC	-0.1139	-0.1092	4.17	3.44
Total	0.4507	0.4500	0.16	0.11
$dd, dd; L = 0$				
FWA (h)	0.3237	0.3234	0.10	0.12
FWA (xc)	-0.0341	-0.0344	0.81	1.81
FWA	0.2897	0.2890	0.24	0.29
SC	-0.0380	-0.0375	1.24	1.37
Total	0.2517	0.2515	0.09	0.05
$sp, sp; L = 1$				
FWA (h)	0.1365	0.1417	3.84	3.91
FWA (xc)	-0.0244	-0.0274	12.12	12.25
FWA	0.1120	0.1144	2.13	2.05
SC	-0.0475	-0.0342	27.91	27.45
Total	0.0645	0.0801	24.25	21.17
$sp, pd; L = 1$				
FWA (h)	0.0935	0.0987	5.56	5.87
FWA (xc)	-0.0160	-0.0178	11.12	12.03
FWA	0.0775	0.0809	4.41	4.58
SC	-0.0331	-0.0254	23.23	22.75
Total	0.0443	0.0555	25.30	22.54
$pp, pp; L = 2$				
FWA (h)	0.0586	0.0606	3.33	3.31
FWA (xc)	-0.0230	-0.0254	10.24	10.51
FWA	0.0356	0.0352	1.13	1.43
SC	-0.0055	-0.0037	32.48	31.92
Total	0.0301	0.0315	4.60	3.87
$dd, dd; L = 2$				
FWA (h)	0.0283	0.0286	1.03	1.09
FWA (xc)	-0.0341	-0.0344	0.81	1.81
FWA	-0.0057	-0.0058	1.49	0.96
SC	-0.0026	-0.0022	15.29	23.91
Total	-0.0083	-0.0080	3.76	8.88

C. From Ar to K

Argon is a rare-gas element. To explore the general trends of the hardness matrix along the Periodic Table, we further calculated the hardness matrix for atoms having a wide range of properties.

We start with Si. To study the effect of core radius r_c on the quality of PSP generated, we plot in Fig. 2 the results for both small and large r_c indicated by dashed and shaded bars respectively (values for r_c are indicated in the captions). The AE results are still plotted with hollow bars. These results are for Si^+ in configuration $s^2p^1d^0$. For small r_c, the PSP hardness elements for Si agree with the AE results very well. (The biggest errors occur for $L = 1$ elements as for Ar.) With the exception of $\{dd, dd; L = 0\}$ elements, a worsening of the agreement in total hardness is evident in the $L = 0$ channel for larger r_c. (The d wave function is nodeless and very delocalized, and thus insensitive to changes in core radius.)

One expects that increasing r_c should always make the PSP less transferable, but the sensitivity can be different for different elements. In Fig. 3, we show a similar diagram for oxygen, again using hashed and shaded bars to represent hardness elements for a PSP with small and

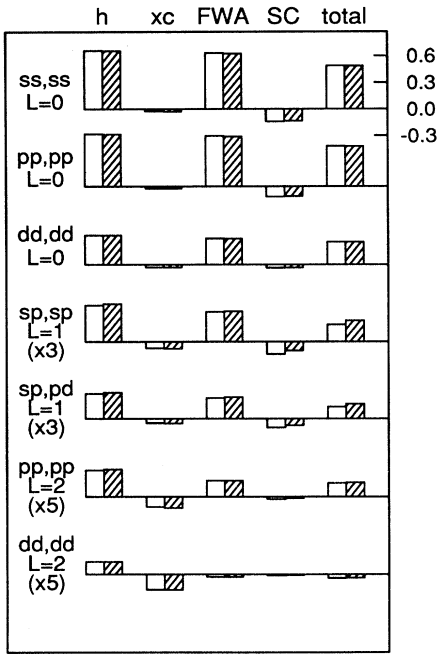

FIG. 1. Magnitudes of some important hardness matrix elements for Ar in configuration $3s^{1.2}3p^{5.7}3d^{0.1}$. The hollow bars represent the all-electron results while the dashed bars represent pseudopotential results at $r_{cs} = 0.9$ a.u., $r_{cp} = r_{cd} = 1.0$ a.u. Different contributions are decomposed into different columns as, "h" (Hartree), "xc" (exchange-correlation), "FWA" (total hardness under frozen wave-function approximation), "SC" (self-consistent correction), and "total" hardness. The $L > 0$ hardness matrix elements are rescaled by a factor of $2L + 1$ to make them more clear.

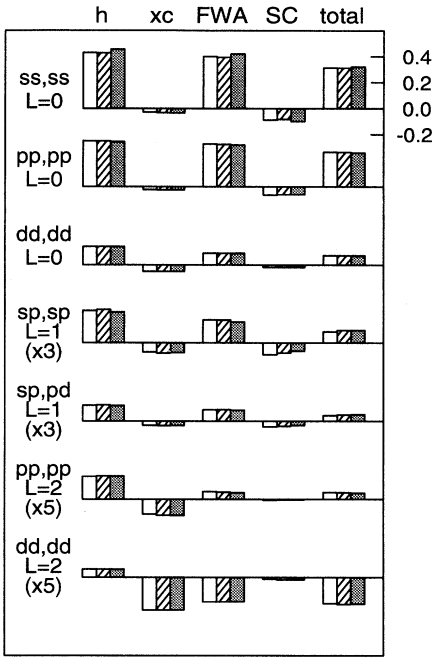

FIG. 2. Hardness matrix elements for Si^{+} in configuration $s^2p^1d^0$. Hollow bars represent AE results, while the dashed and shaded bars represent PSP results at $r_{cs} = 1.1$ a.u., $r_{cp} = 1.2$ a.u., $r_{cd} = 0.8$ a.u., and $r_{cs} = 2.3$ a.u., $r_{cp} = 2.4$ a.u., $r_{cd} = 0.8$ a.u., respectively.

large r_c. We find that the effect of increasing r_c is more dramatic for O. A more complete picture of the effect of r_c will be presented later.

We next focus on a couple of cases to characterize the role of the LFC correction.[6] In the following figures, we use the shaded bars to represent PSP results with such LFC correction. The results we presented are for $K^{+0.25}$ in $s^{0.25}p^{0.25}d^{0.25}$ (Fig. 4) and $Ti^{+0.75}$ in configuration $s^1p^{0.25}d^2$ (Fig. 5). For K, we find that the LFC greatly reduces the error due to the H^{xc} contribution to the hardness matrix elements even for the $L = 0$ channel. The LFC-corrected hardness matrices are in good agreement with the AE results. For Ti, the LFC successfully corrects the noticeable mismatch between AE and no-LFC results for H^{xc} contributions to the $\{dd, dd; L = 0\}$ and $\{dd, dd; L = 2\}$ elements. (The no-LFC total hardness in the $\{dd, dd; L = 0\}$ happens to match the AE one rather closely, but only because of a fortuitous cancellation of errors.)

The hardness results obviously depend on details of the PSP construction, but we note the following general trends. In going from left to right across a row of the Periodic Table, an increasing atomic number tends to localize the core density closer to the nucleus and to reduce the size of the core. Consequently, the overlap between core and valence charge densities, which is the source of the nonlinearity in the exchange-correlation potential, gets smaller and smaller. Such an overlap, when significant, is largely responsible for the errors in the self-consistent contribution to hardness as well, i.e., for

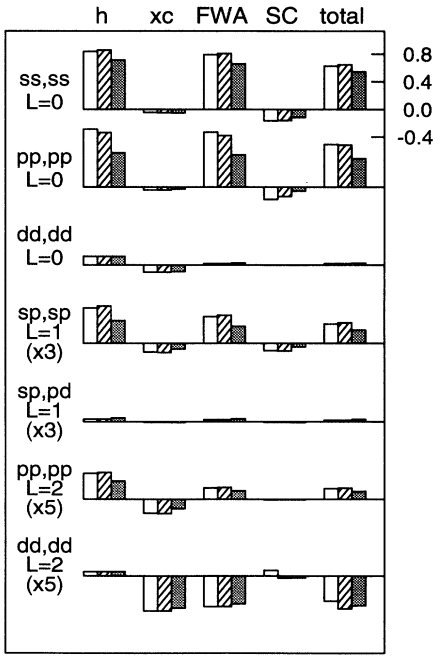

FIG. 3. Hardness matrix elements for O in configuration $s^{1.4}p^{3.5}d^{0.1}$. Hollow bars represent AE results, while the dashed and shaded bars represent PSP results at $r_{cs} = 0.8$ a.u., $r_{cp} = 0.9$ a.u., $r_{cd} = 0.8$ a.u., and $r_{cs} = 2.9$ a.u., $r_{cp} = 3.0$ a.u., $r_{cd} = 0.8$ a.u., respectively.

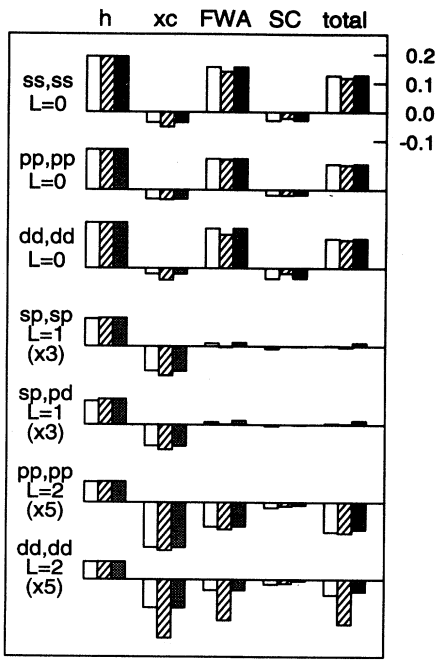

FIG. 4. Hardness matrix elements for K in configuration $s^{0.25}p^{0.25}d^{0.25}$. Hollow bars represent AE results, while the dashed and shaded bars represent PSP results ($r_{cs} = 1.8$ a.u., $r_{cp} = 2.3$ a.u., and $r_{cd} = 1.2$ a.u.) without and with the LFC partial-core correction, respectively.

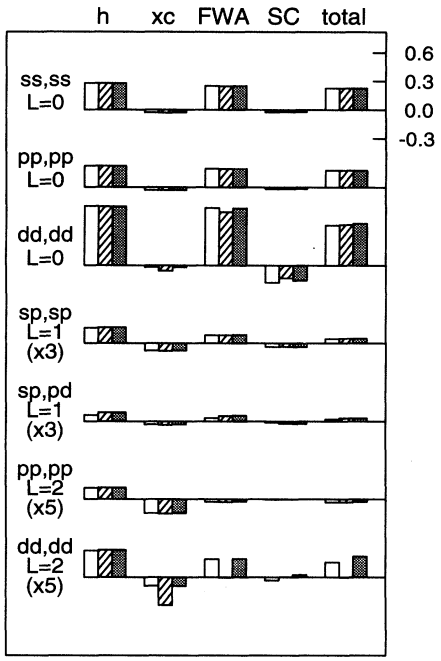

FIG. 5. Hardness matrix elements for Ti in configuration $s^1p^{0.25}d^2$. Hollow bars represent AE results, while the dashed and shaded bars represent PSP results ($r_{cs} = 1.8$ a.u., $r_{cp} = 2.3$ a.u., and $r_{cd} = 0.8$ a.u.) without and with the LFC partial-core correction, respectively.

a poor description of the rearrangement of the pseudo-wave-functions. Provided that one takes small core radii to minimize errors in the Hartree contributions, the degree of core-valence overlap almost entirely determines the PSP transferability. Rare-gas atoms thus have maximum transferability without LFC, while alkali atoms need the LFC correction the most.

Moving along the *columns* of the Periodic Table, the trends are naturally much weaker. In fact, the net positive charge seen by the valence electrons is nearly the same. However, a slight increase of overlap occurs, along with a corresponding loss of transferability of non-LFC PSP, as one goes down the columns.

From our hardness matrix results, we can investigate whether there is a systematic way to improve the PSP transferability. The Hartree contribution can be improved by imposing additional conditions on the pseudo-wave-functions, e.g., matching of the valence electrostatic potentials for higher-order multiple moments.[22] However, it is not clear whether the gain in transferability would justify the drawbacks of imposing additional constraints. As regards the exchange-correlation terms, while some other approaches have been tried,[23] the LFC correction seems to be the simplest and most efficient method.

D. Average hardness errors

We have shown that it is useful to characterize the transferability of a PSP in terms of its hardness matrix. However, there is so much information contained in the numerous matrix elements of the hardness matrix that it becomes difficult to decide whether a particular PSP shows "good" or "poor" transferability. Thus, it is desirable to define a single quantity that can be used to represent approximately the overall transferability of the PSP. There is certainly no unique way to do this, since the importance of different matrix elements depends on the target application. Nevertheless, we propose one such definition, which at least can be used as a starting point.

We define an average hardness error X as follows:

$$X^2 = \sum_{\alpha\beta L} w_{\alpha\beta L} \, (\Delta H_{\alpha\beta L})^2 \, . \tag{32}$$

Here ΔH is the difference between total AE and PSP hardness matrix elements, and $w_{\alpha\beta L}$ is a weight to be defined shortly. Thus, X is just a weighted rms average of the errors in the hardness matrix elements.

To fix the weights $w_{\alpha\beta L}$, we have adopted the following philosophy. We want X to represent an average total-energy error that would occur as the PSP atom is transferred to an ensemble of target environments, where the distribution of target environments is characterized by specifying the average occupation N_l and the typical fluctuation in occupation η_l, for each electron shell. In the spirit of the hardness approach, we can estimate the change in total energy of the atom as it is inserted into a given environment as

$$\Delta E = \sum_{\alpha\beta LM} H_{\alpha\beta L} \, \delta f_{\alpha LM} \, \delta f_{\beta LM} \, . \tag{33}$$

If each contribution were statistically independent, one would have

$$(\Delta E)^2 \simeq (2L+1) \sum_{\alpha\beta L} H^2_{\alpha\beta L} \, \delta f^2_{\alpha LM} \, \delta f^2_{\beta LM} \, . \tag{34}$$

To make things simple, we assume that the fluctuation η_l is a function only of the average occupation N_l and the maximum occupation $2(2l+1)$ of the shell. We choose the form

$$\eta_l = (2l+1) \sqrt{2 f_l (1 - f_l)} \, , \tag{35}$$

where f_l is the fractional occupancy, $f_l = N_l/2(2l+1)$. The first term makes the fluctuation proportional to the number of electrons that could be accommodated in the shell; the second forces the fluctuation to zero for either a completely filled or a completely empty shell in a manner that respects electron-hole symmetry. Making the additional rough approximation that $\delta f^2_{\alpha LM} \propto \eta_{l_\alpha} \eta_{l'_\alpha}$ and $\delta f^2_{\beta LM} \propto \eta_{l_\beta} \eta_{l'_\beta}$ (where $\alpha = n_\alpha n'_\alpha l_\alpha l'_\alpha$ and the n subscripts are suppressed) and replacing $(H_{\alpha\beta L})^2$ by the AE versus PSP error $(\Delta H_{\alpha\beta L})^2$, we arrive at the right-hand side of Eq. (32) with

$$w_{\alpha\beta L} = (2L+1) \, \eta_{l_\alpha} \, \eta_{l'_\alpha} \, \eta_{l_\beta} \, \eta_{l'_\beta} \, . \tag{36}$$

Thus, we have defined X through Eqs. (32), (36), and (35), in such a way that it depends only on a specifica-

tion of the reference electronic configuration (the N_l values). Our definition puts no weight on completely filled or completely empty shells, and heavily weights partially filled shells.

We would be the first to admit that the choices above are largely arbitrary, but we believe they are reasonable ones, and we proceed to use this measure to study the effect of variations in core radius upon PSP transferability. In Figs. 6 and 7, we show the calculated average hardness error X for a set of six elements as a function of $r_c = (r_{cs} + r_{cp})/2$. Here, $r_{cp} - r_{cs}$ is kept constant. We do not change r_{cd}, since it does not affect X appreciably for the atoms studied here (with no d electrons inside the core). The hardness error X (and the hardness itself) is much greater for first-row elements C and O, so they are plotted on a different scale. It can be seen that the behavior of X differs considerably between elements. For K (with LFC correction), X is very insensitive to r_c, and there is thus wide flexibility in the choice of an appropriate r_c. For O, C, and Ga, X increases in an approximately linear fashion as r_c is increased from 1.5 to 3.5 au, while X increases more rapidly for Si and Ar as r_c is increased.

E. Polarizability

In Table III, we show our calculated dipole ($L = 1$) and quadrupole ($L = 2$) polarizability for some AE and PSP atoms. Our AE results for rare-gas and closed-shell ions agree very well with previous calculations.[14,24,25] The results for the dipole polarizability are also in good agreement with experiment. (Experimental values for higher-moment polarizability do not appear to be available.) For example, for the K^+ ion, we find the dipole susceptibility to be 5.74 a.u., compared to 5.86 a.u. and 5.47 a.u. from previous theory[14] and the experiment,[26] respectively. Note that most of the results reported below are for open-shell atoms or ions. It should be emphasized that in these cases, our results are a theoretical fiction in that we assume symmetrized occupations (e.g., $s^2 p_x^{2/3} p_y^{2/3} p_z^{2/3}$ for C) that have little relation to the real atomic ground state. Nevertheless, we believe it is meaningful to compare AE and PSP polarizability calculated in this way as a means of testing the transferability of a PSP. We tend to prefer tests on ionized configurations (e.g., Si^+ instead of Si) because we have found that shallow orbitals in neutral open-shell atoms sometimes give such enormous contributions to the polarizability that comparison becomes difficult. All PSP's are built choosing small core radii (e.g., $r_{cs} = 1.1$ a.u. for Si^+), and for K the LFC correction was used.

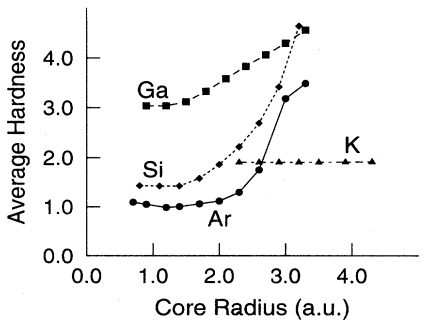

FIG. 6. Calculated average hardness error for Ar, Si, Ga, and K as a function of core radius used in the PSP generation. The configurations used to calculate the average hardness errors are Ar ($3s^{1.95}3p^{5.95}3d^{0.05}$), Si ($3s^{1.2}3p^{2.7}3d^{0.1}$), Ga ($4s^{1.2}4p^{1.7}3d^{0.1}$), and K ($4s^{0.85}4p^{0.1}3d^{0.05}$). The LFC partial-core correction was employed only for K.

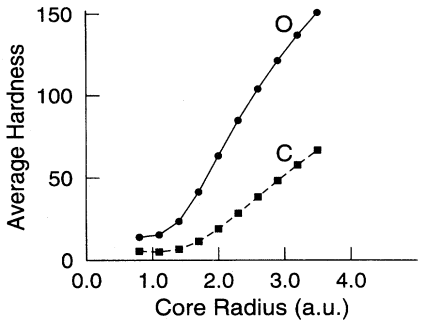

FIG. 7. Calculated average hardness error for C and O as a function of core radius used in the PSP generation. The configurations used to calculate the average hardness errors are C ($2s^{1.9}2p^{2.0}3d^{0.1}$) and O ($2s^{1.5}2p^{4.0}3d^{0.5}$). The LFC partial-core correction was not employed.

We first consider the all-electron results. To test the effect of self-consistent screening, we report both FWA and SC polarizabilities. All pseudopotentials are built choosing small core radii, and for potassium, the LFC correction is used. In all cases, the core polarizability is included in the all-electron value. As a example, we show the core contribution of K^+ to its all-electron polarizability.

Looking at Table III, it is evident that only the dipole polarizability is strongly affected by self-consistent screening. The screening reduces the dipole polarizability by around 40%, while the quadrupole susceptibility is typically reduced by only about 3%. Exceptions to this pattern occur for some highly polarizable atoms like potassium, for which the screening correction is still sizeable in the quadrupole channel.

Three factors contribute to the difference between PSP and AE polarizability: (i) the core contribution; (ii) the difference between unperturbed pseudo- and AE wave functions inside the core region; and (iii) differences in the first-order changes in the valence wave functions. Regarding (iii), the wave function changes are determined in part by admixture of angular-momentum components higher than those which are present in the unperturbed reference configuration. For these components (typically $l \geq 3$), no norm-conservation or tail-matching conditions were imposed. Because the PSP usually contains no nonlocal projectors for large l, these wave functions feel only the local potential, which is usually set in a very arbitrary manner. This appears to be the most significant

TABLE III. Comparison between all-electron (AE) and pseudopotential (PSP) dipole and quadrupole polarizability in atomic units ($e^2 = 2$) for selected ions.

	Frozen-wave approximation			Self-consistent results		
	AE	PSP	error (%)	AE	PSP	error (%)
Dipole						
K^+	8.89			5.74		
$K^{+0.3}$ $(s^{0.7})$	181.94	175.76	3.4	165.89	164.83	0.6
C^+ (s^2p^1)	10.04	10.16	1.2	6.04	6.04	0.0
$Ar^{+0.5}$ $(s^2p^{5.5})$	13.82	13.93	0.8	9.01	9.02	0.2
Si^+ (s^2p^1)	31.61	31.82	0.7	19.11	19.19	0.4
$Ga^{+0.5}$ $(s^{2.0}p^{0.5})$	46.97	45.12	3.9	29.60	29.97	1.2
Ge^+ (s^2p^1)	30.38	29.60	2.6	18.93	19.12	0.9
Ti^+ $(s^2p^0d^1)$	90.50	90.61	0.1	47.98	48.26	0.6
Quadrupole						
K^+	18.7			18.2		
$K^{+0.3}$ $(s^{0.7})$	2530	2521	0.3	3044	3029	0.5
C^+ (s^2p^1)	16.4	16.4	0.0	16.8	16.8	0.0
$Ar^{+0.5}$ $(s^2p^{5.5})$	38.2	38.2	0.0	37.8	37.8	0.0
Si^+ (s^2p^1)	107.5	107.5	0.0	108.2	108.3	0.1
$Ga^{+0.5}$ $(s^{2.0}p^{0.5})$	220.1	218.8	0.6	228.5	228.1	0.2
Ge^+ (s^2p^1)	107.4	106.7	0.7	108.9	108.5	0.3
Ti^+ $(s^2p^0d^1)$	301.8	286.8	5.0	319.9	316.1	1.2

source of error in PSP polarizability. For example, we have calculated the PSP polarizability of Ar both with and without an f component in the nonlocal projector. We find that the calculated values for both the dipole and quadrupole polarizabilities are about 15% too small when the f component of the projector is omitted. This effect was already noted in Ref. 17, where many other examples can be found. All the results in Table III are obtained using a PSP with a complete projector (up to $l = 3$).

The results in the table indicate that while the screening correction generally improves the agreement between AE and PSP for the dipole susceptibility, the error in the quadrupole susceptibility is almost unaffected. Generally, we find a very good agreement between the self-consistent AE and PSP results. However, it should be noted that all results shown in the table were obtained using a PSP generated from the same configuration for which the polarizability calculation was made. If we change the PSP reference configuration considerably, larger changes in the calculated PSP polarizability may occur.

IV. CONCLUSION

We present a systematic method for characterizing the transferability of pseudopotentials using their linear-response properties, specifically their generalized chemical hardness, and dipole and quadrupole polarizabilities. The hardness measures the ability of the PSP to resemble the all-electron atom in different atomic environments, including nonspherical ones, while the polarizabilities reflect the response of the PSP atom to external fields. When used together with conventional criteria such as norm-conservation and matching of eigenvalues and logarithmic derivatives, this approach allows a rather complete characterization of PSP transferability.

We have applied the method to study the behavior of Hamann-Schlüter-Chiang pseudopotentials for many atoms in the Periodic Table. As expected, the calculated hardness matrix indicates that the transferability deteriorates as the core radius is increased. For some elements with relatively delocalized cores, we find strong evidence for the importance of including the Louie-Froyen-Cohen semicore correction. We propose a method for reducing the large amount of information contained in the hardness matrix to a single number. We suggest that this quantity be monitored or included in the fitting procedure when generating pseudopotentials, in order to achieve the desired properties (e.g., optimal smoothness) without sacrificing transferability.

ACKNOWLEDGMENTS

D.V. and W.Z. gratefully acknowledge support from NSF Grant No. DMR-91-15342 and ONR Grant No. N00014-91-J-1184. A.F. and G.B.B. acknowledge support from the Progetto Finalizzato Sistemi Informatici e Calcolo Parallelo of the Italian National Research Council, CNR Grant Nos. 89.0006.69 and 89.00051.69. A.F. also thanks R. W. Nunes for his kind help and the Department of Physics and Astronomy of Rutgers University for its warm hospitality during part of this project.

* Permanent address: Prudential Securities Inc., 1 New York Plaza, New York, NY 10006.
[1] P. Hohenberg and W. Kohn, Phys. Rev. **136**, B864 (1964); W. Kohn and L. J. Sham, *ibid.* **140**, A1133 (1965).
[2] For an excellent review, see W. E. Pickett, Comput. Phys. **9**, 115 (1989).
[3] D. R. Hamann, M. Schlüter, and C. Chiang, Phys. Rev. Lett. **43**, 1494 (1979).
[4] G. B. Bachelet, D. R. Hamann, and M. Schlüter, Phys. Rev. B **26**, 4199 (1982).
[5] S. Goedecker and K. Maschke, Phys. Rev. A **45**, 88 (1992).
[6] S. G. Louie, S. Froyen, and M. L. Cohen, Phys. Rev. B **26**, 1738 (1982).
[7] D. Vanderbilt, Phys. Rev. B **32**, 8412 (1985).
[8] A. M. Rappe, K. M. Rabe, E. Kaxiras, and J. D. Joannopoulos, Phys. Rev. B **41**, 1227 (1990).
[9] N. Troullier and J. L. Martins, Phys. Rev. B **43**, 1993 (1991).
[10] M. Teter, Phys. Rev. B **48**, 5031 (1993).
[11] J. F. Janak, Phys. Rev. B **18**, 7165 (1978).
[12] D. Vanderbilt and J. D. Joannopoulos, Phys. Rev. B **26**, 3203 (1982).
[13] X.-P. Li, R.W. Nunes, and D. Vanderbilt, Phys. Rev. B **47**, 10 891 (1993).
[14] G. D. Mahan and K. R. Subbaswamy, *Local Density Theory of Polarizability* (Plenum Press, New York, 1990).
[15] A. Filippetti, Tesi di Laurea, Università la Sapienza, Rome, 1994.
[16] J.O. Eaves and S.T. Epstein, J. Chem. Phys. **61**, 3486 (1974).
[17] G. B. Bachelet, C. Tanner, and M. Schlüter, Phys. Status Solidi B **110**, 313 (1982).
[18] G. D. Mahan, Phys. Rev. A **22**, 1780 (1980).
[19] G. P. Kerker, J. Phys. C **13**, L189 (1980).
[20] L. Kleinman and D. L. Bylander, Phys. Rev. Lett. **48**, 1425 (1982).
[21] D. Vanderbilt, Phys. Rev. B **41**, 7892 (1990).
[22] E. L. Shirley, D. C. Allan, R. M. Martin, and J. D. Joannopoulos, Phys. Rev. B **40**, 3652 (1989).
[23] D. L. Bylander and L. Kleinman, Phys. Rev. B **43**, 12 070 (1991).
[24] A. Zangwill and P. Soven, Phys. Rev. A **21**, 1561 (1980).
[25] M. J. Stott and E. Zaremba, Phys. Rev. A **21**, 12 (1980).
[26] R. R. Freeman and D. Kleppner, Phys. Rev. A **14**, 1614 (1976); J. C. Lombardi, *ibid.* **36**, 1445 (1987).